

# Graphene-based spinmechatronic valve

Ali Hallal

*Univ. Grenoble Alpes, CEA, CNRS, Spintec, 38000 Grenoble, France\**

Interlayer twist between van der Waals graphene crystals led to the discovery of superconducting and insulating states near the magic angle. In this work, we exploit this mechanical degree of freedom by twisting the graphene middle layer in a trilayer graphene spacer between two metallic lead (Magnetic and nonmagnetic). A large difference in conductance is found depending on the angle of twist between the middle layer graphene and the ones at the interface this difference, called twisting resistance, reach more than 1000% in the non-magnetic Cu case. For the magnetic Ni case, the magneto-resistance decreases and the difference in conductance between twisted and not twisted depends strongly on the relative magnetization configuration. For the parallel configuration, the twisting resistance is about -40%, while for the anti-parallel configuration it can reach up to 130%. Furthermore, we show that the twisting resistance can be enhanced by inserting a thin Cu layer at the interface of Ni/graphene where it reaches a value of 200% and 1600% for parallel and antiparallel configurations, respectively. These finding could pave the way toward the integration of 2D materials on novel spinmechatronics based devices.

Graphene incorporation in magnetic tunnel junctions (MTJs) [1–4] has attract a lot of attention recently due to its protective nature against the oxidation of the ferromagnetic layer [5]. In addition graphene multilayers are found to be a perfect spin filter in vertical magnetic tunnel junctions [6–8]. Furthermore, and despite its weak spin-orbit coupling (SOC), graphene coating of Co is found to induce a large perpendicular magnetic anisotropy [9–12] and a significant Dzyaloshinskii-Moriya interaction due to the Rashba effect [13–15]. In addition, graphene-based magnetic multilayers show a strong perpendicular anti-ferromagnetic exchange coupling that could be used as synthetic anti-ferromagnetic [16, 17]. Those findings have promoted graphene, and subsequently other two dimensional (2D) materials, as potential candidates to replace oxide barrier in conventional MTJs.

The weak coupling between different layers of 2D materials allows to manipulate the relative twisting angle (RTA) between two or more layers of graphene leading to the formation of moiré superlattices. The electronic properties of such herterostructure strongly depend on the RTA between two or more layers. This led recently to the discovery of superconductivity [18–21], insulating state [22–25], and even orbital ferromagnetism [26, 27] near the "magic angle" in twisted bilayer graphene (TBLG). Furthermore, recent experiment show the possibility to control in-situ [28] the RTA and thus giving rise to a mechanical degree of freedom led to an emerging field called twistronics. The transport properties of TBLG [29–31] and bilayer graphene nanoribbons [32] has been lately investigated in lateral geometry show a strong effect of the RTA on the electric properties of the system. A scientific investigation of transport properties in vertical geometry is still lacking. Incorporating graphene in MTJ and varying the RTA will strongly affects the electronic properties of MTJs; a procuration which is not possible using conventional oxide structures.

In this work, using first principle calculations, we demonstrate a significant difference in resistance between non-twisted and twisted tri-layer graphene (TTLG) spacer, we call as twisting-resistance (TwR), between two metallic leads (magnetic or non-magnetic). In case of non-magnetic Cu substrate, the TwR could reach more than 1000% which is attributed to the absence of conducting state in large region around the K point in reciprocal space. Once the middle layer of graphene is twisted, it start to feel the populated states present round the M point and thus a large current go through the graphene layer. For the magnetic Ni case, the current are mostly dominant by the minority electrons for parallel configuration as explained and shown earlier by V. M. Karpan et. al. [6], leading to perfect spin filter. Rotating the middle layer lead to a reduction of the spin filter effect due to the increase of majority conductance.

First, we start by examining the transmission map across the Brillouin zone at Fermi level for pure Cu film as shown in Fig. 1 (a) (left panel), the current passes homogeneously throughout the reciprocal space except at the edges where there is no state available. In the other hand, graphene or graphite the only state close to Fermi energy are found near the high symmetry K point in reciprocal space. So if we put graphene or graphite in top of Cu the electrons will have to overcome a large barrier to tunnel Fig. 1 (a) (middle panel). However, if graphene layer is twisted by an angle of  $30^\circ$  the Dirac cone of graphene are now in top or close to the region where the Cu have high transmission probability and thus the electrons will go through easily. For a ferromagnetic case, such as Ni or Co, the only states are present around the K point are the minority spin character while for majority spin case the transmission map is similar to that of Cu and this fact is at the origin of large spin filtering effect in Fm/graphite/FM (FM = Ni or Co) [c.f. Fig. 1 (b)]. Similarly, If graphene layer in top of Ni is twisted we expect the Majority current will enhance and that of

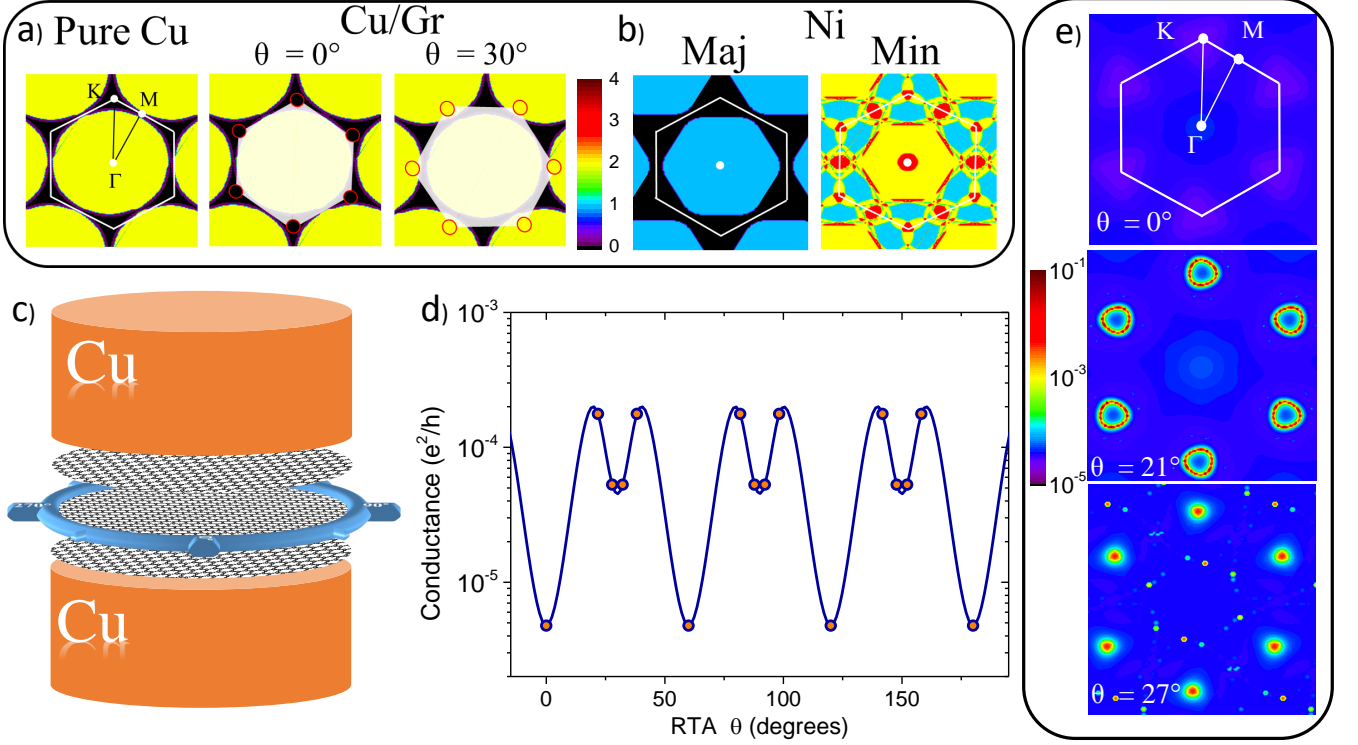


FIG. 1. (a) (left panel) Transmission map across the Brillouin zone of Pure Cu, middle and right panel show a schematic of graphene Fermi surface in top of Cu transmission map with a RTA angle of  $0^\circ$  and  $30^\circ$ , respectively. (b) Majority and minority transmission map across the Brillouin zone of Ni. (c) Schematic of the proposed device composed of Cu/TTLG/Cu junction where the middle layer of graphene could be twisted relative to the ones at the interfaces. (d) Quantum conductance at room temperature of Cu/TTLG/Cu as function of the RTA. (e) top middle and bottom show transmission map across Brillouin zone at Fermi energy for RTA of  $0^\circ$ ,  $21.787^\circ$  and  $27.8^\circ$ , respectively. The Brillouin zone with high symmetry points are shown in white.

the minority will decreases.

To verify our hypothesis and to investigate the effect of RTA on the electronic transport properties in vertical graphene-based junctions, we setup a structure of Cu/TTLG/Cu, where only the middle layer graphene is rotated relative to the graphene layers at the interface as shown in Fig. 1 (c). There are two types of twisted layer of graphene in the literature the commensurate and non-commensurate [33, 34] in this paper we focus on the commensurate twisted layer graphene. Due to computational limitation we can only study two relative rotation angles (RTA) of commensurate twisted graphene that have the smallest possible unit cell. The two RTA we study are  $21.787^\circ$  and  $27.8^\circ$  that correspond to a unit cell of  $\sqrt{7} \times \sqrt{7}$  and  $\sqrt{13} \times \sqrt{13}$ , respectively. Due to the six fold symmetry of graphene, the  $21.787^\circ$  and  $27.8^\circ$  is similar to that of  $38.213^\circ$  and  $32.2^\circ$ . The in-plane lattice constant and the interlayer distance between graphene and substrate are taken from ref. [6] The scattering region is composed of trilayer of graphene sandwiched between 6 layers of Cu or Ni and attached to 6 layers of Cu or Ni lead.

Our first-principles calculations were performed using

SIESTA package [35, 36] and the exchange correlation energy calculated within the generalized gradient approximation of Perdew-Burke-Ernzerhof (PBE) [37] and valence states were expanded by numerical atomic orbital basis sets with Single-zeta (SZ) functions. Atomic cores were described by non-local norm conserving Troullier-Martins pseudopotentials. The cutoff energy is set to 300 Ry and found to be more than sufficient in our case. For RTA of  $21.787^\circ$  ( $32.2^\circ$ ) Monkhorst-Packgrids of  $7 \times 7 \times 1$  ( $3 \times 3 \times 1$ ) and  $7 \times 7 \times 20$  ( $3 \times 3 \times 20$ ) k-points were used for the Brillouin zone integration of the device and electrodes, respectively. Nonequilibrium Green function (NEGF) transport calculation were performed using TranSIESTA [38, 39] to study spin-dependent transport. For transmission calculation a  $100 \times 100 \times 1$  and  $50 \times 50 \times 1$  is used for RTA of  $21.787^\circ$  and  $32.2^\circ$  using the TBTrans code, respectively.

In general the twisting magneto-resistance can be defined as the difference between two conducting state with/without different twisting angle and/or different magnetization orientation, as following:

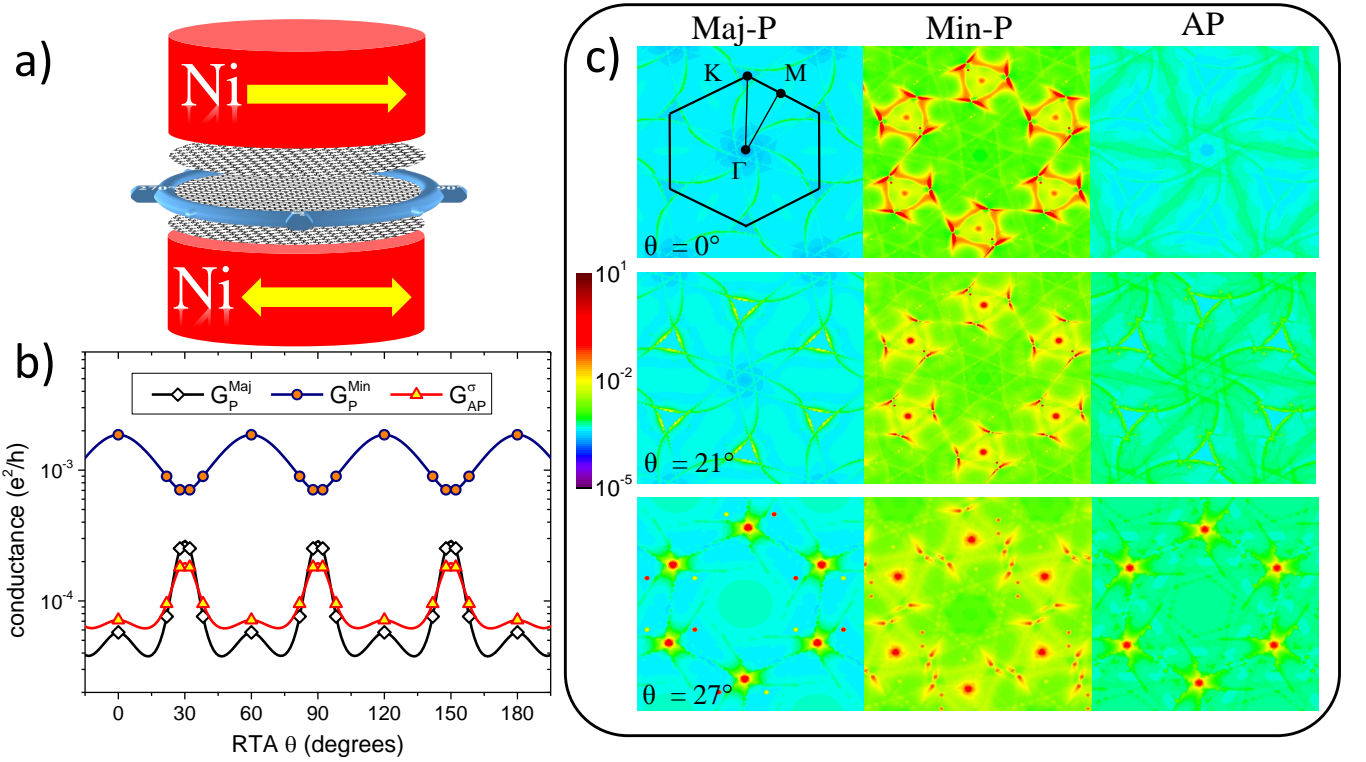


FIG. 2. (a) Device schematic composed of Ni/TTLG/Ni where the middle layer graphene is rotated relative to the ones at the interface. (b) Majority, minority conductance for parallel and anti-parallel configurations of Ni/TTLG/Ni MTJs at room temperature as function of the RTA. (c) Transmission map across Brillouin zone at Fermi energy for majority parallel (left), minority parallel (middle) and anti-parallel (right) for RTA of  $0^\circ$  (top),  $21.787^\circ$  (middle) and  $27.8^\circ$  (bottom).

$$\left(\frac{\Delta G}{G}\right)_{\alpha, \alpha'}(\theta, \theta') = \frac{G_\alpha(\theta) - G_{\alpha'}(\theta')}{G_{\alpha'}(\theta')}$$

Where,  $\theta$  and  $\alpha$  represent the RTA and magnetization configuration, namely parallel (P) or anti-parallel (AP), respectively. In this case, the magneto-resistance (MR) is nothing but  $MR(\theta) = \left(\frac{\Delta G}{G}\right)_{\alpha, -\alpha}(\theta)$  where the RTA is fixed and the magnetization direction ( $\alpha$ ) is changed from P to AP. Similarly, the Twisting resistance is nothing but  $TwR_\alpha = \left(\frac{\Delta G}{G}\right)_\alpha(\theta, \theta')$  where the magnetization direction is fixed either to parallel or anti-parallel and the RTA is varied.

Next, we discuss the non-magnetic case (Cu/TTLG/Cu) by looking at the variation of quantum conductance at Fermi energy and at room temperature as function of RTA ( $\theta$ ) as shown Fig. 1 (d). The conductance show an increases of almost two order of magnitude for RTA of  $21.787^\circ$  compared to the non-twisted case and then slightly decreases for  $\theta = 27.8^\circ$ . The estimated TwR are found to be about 3600% and 1000% for RTA of  $21.787^\circ$  and  $28.7^\circ$ , respectively. These large values, comparable to the tunneling magento-resistance found in Fe/MgO MTJs, pave the way towards using the mechanical degree of freedom in

storage and logic devices. To understand the origin of these large values we plot in Fig. 1 (e) the Transmission profile across the Brillouin zone for different angles. For the non-twisted case, the Transmission are quite homogeneous across the Brillouin zone except at the high symmetry point K where the conductance is minimal. This behavior is expected since the pure Cu have no state present at these states as shown in Fig. 1 (a). As the middle graphene layer is rotated the transmission probability at K-point become maximal and contribute strongly to the conductance ( c.f. Fig. 1 (e) middle and bottom panel).

For the magnetic case, i.e in Ni/TTLG/Ni junctions (Fig. 2 (a)), the transport properties are influenced by the relative magnetizations configuration in addition to the mechanical degree of freedom arising from the TTGL spacer. The conductance in case of majority ( $G_P^{Maj}$ ), minority parallel( $G_P^{Min}$ ) and anti-parallel( $G_{AP}^\sigma$ ) configuration are shown in Fig. 2 (b) as function of RTA  $\theta$ . In the anti-parallel case, ( $G_{AP}^\sigma$  increases with increasing the RTA angle where it reach maximum around  $30^\circ$ . Interestingly,  $G_P^{Maj}$  ( $G_P^{Min}$ ) show a similar (opposite) behavior to that of  $G_{AP}^\sigma$  where it increases (decreases) as RTA increases from  $0^\circ$  to  $30^\circ$ . Thus, the overall parallel conductance is less effected by the RTA

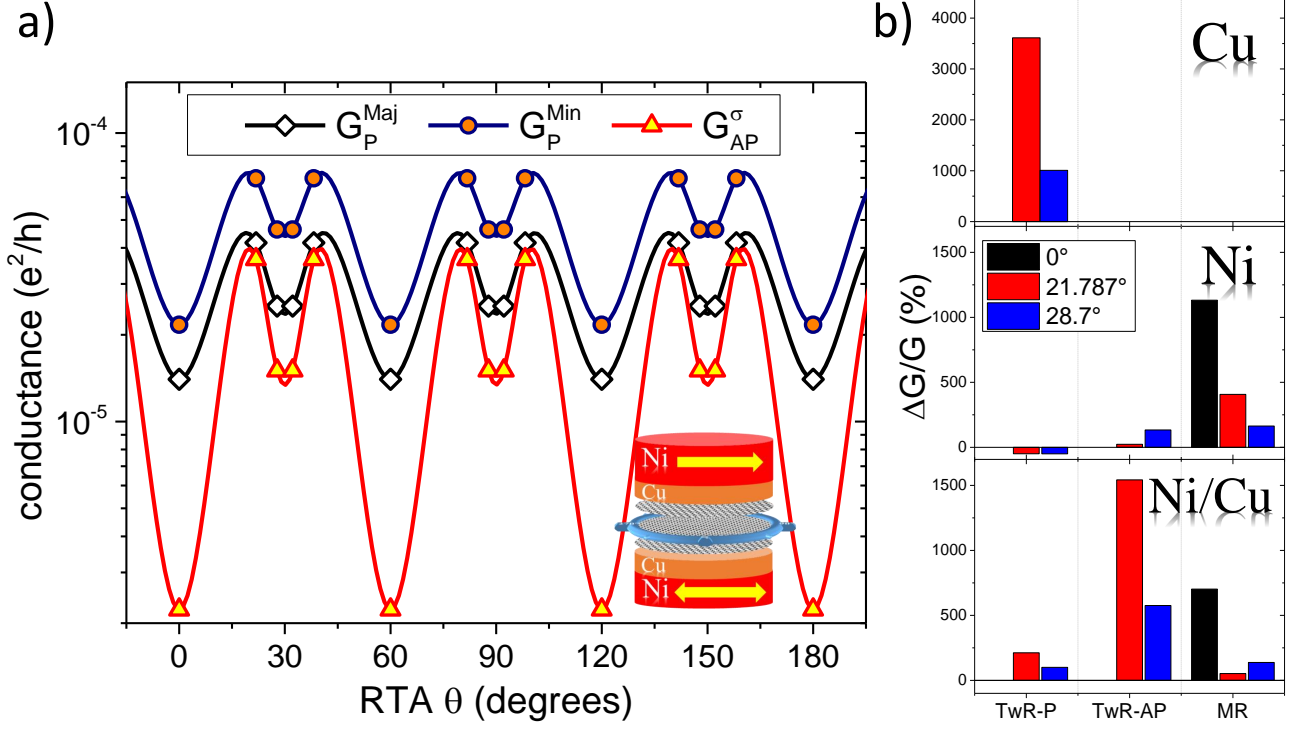


FIG. 3. (a) Majority parallel, minority parallel and anti-parallel conductances of Ni/Cu(3ML)/TTLG/Cu(3ML)/Ni MTJs at room temperature as function of the RTA with a schematic of the device is shown in the inset. (b) twisting magneto-resistance of the parallel and anti-parallel configurations with different RTA for the different investigated metallic substrate, Cu (top), Ni (middle), and Ni/Cu (bottom).

compared to the antiparallel case leading to a decrease by one order of magnitude of MR from 1000% at RTA =  $0^\circ$  to 163% at RTA =  $27.8^\circ$ . Therefore, the spin filtering effect of graphite is sensitive to the relative rotation angle of its layer. The magnitude of TwR found in case of Ni is much smaller than that found in Cu substrate. However, the sign of TwR depends on the alignment of magnetizations, if it parallel TwR < 0 and if they are anti-parallel TwR is > 0. The transmission profile for majority parallel, minority parallel, and anti-parallel configuration at Fermi energy across the Brillouin zone for different angles is plotted in Fig. 2 (c). Similar to the Cu case, the most pronounced changes as function of RTA occurs around the special point in Brillouin zone K. For RTA =  $0^\circ$ , as expected and shown previously in the literature the transmission probability in the parallel configuration is mostly dominated by the spin-down channel (Min-P) around the K point. For the spin-up channel (Maj-P) the transmission probability across the Brillouin zone is quite negligible compared to that of Min-P. This lead to the predicted perfect spin filtering effect in graphene based tunnel junction. For RTA  $\neq 0^\circ$  the Dirac point of the middle layer is not anymore positioned in top of the K point of the Ni. Thus in this case, the transmission of Maj-P and AP will increase while that

of Min-P will decreases around the K point as shown in Fig. 2 (c) left, right, and middle panel, respectively.

To enhance the TwR in the Ni/TTLG/Ni case, we propose to introduce a thin Cu film at the interface between Ni and Gr which will increase the TwR without affecting too much the MR. Fig. 3 (a) show the conductance at room temperature as function of RTA for Ni/Cu(3ML)/TTLG/Cu(3ml)/Ni. Overall the insertion of Cu film decreases the conductivity of the system by one order of magnitude, and unlike pure Ni case the  $G_P^{Min}$  show an increase in conductance value as function of RTA. The latter change of behavior led to increases and changes the sign of TwR in the parallel configuration from negative to positive values where TwR-P in this case is about 200% ( c.f. Fig 3). Moreover, the twisting-resistance in the anti-parallel configuration (TwR-AP) is one order of magnitude larger than the case where no Cu inserted and reaches a values of 1542% and 575% for RTA of  $21.78^\circ$  and  $27.8^\circ$ , respectively. At the same time, the MR decreases to more than one order of magnitude from 700% at  $\theta = 0^\circ$  to 52% at  $\theta = 21.787^\circ$ . This indicate that the spin-filtering effect of graphene based MTJs are strongly effected by the crystal structure and orientation of the spacer.

These findings are promising for next generation

sensor and MTJs based on 2D materials with novel mechanism. One of the challenges in such devices is to control the RTA at the nanoscale in twisted multi-layer graphene. Recent experimental work showed the possibility to modify the RTA in-situ with an atomic force microscope tip [28], however the transition speed is slow for plausible applications. Other alternative is to use optical nano-tweezers to trap a graphene layer and twisted with respect to substrate, recently graphene trapping is achieved at the microscale using optoelectronic tweezer [40]. With the fast developing research of nano-optical tweezer by trapping and rotating nanostructures [41, 42], the possibility to control RTA of multi layer graphene at the nanoscale should be within the reach in the few next years. Finally, theoretical work predicted that thin topological insulator with broken inversion symmetry might experience a torque or "twisting force" [43] as nonequilibrium response to temperature difference with the environment. This phenomena could be used to control efficiently the mechanical degree of freedom in graphene based-MTJs.

In conclusion, we demonstrate, Using spin-dependent transport calculations, the mechanical control of electric current by twisting the graphene middle layer in a trilayer graphene spacer between two metallic leads (magnetic and non-magnetic). A large difference in conductance has been found between two RTA where the TwR could reach more than 1000% for Cu/TTLG/Cu junctions. For the Ni/TTLG/Ni case, we show that the magneto-resistance decreases when the middle layer is twisted with respect to those at the interface, and the TwR depends strongly on the relative magnetization configuration. For the parallel configuration, the TwR is about -40%, while for the anti-parallel configuration it can reach up to 130%. Furthermore, we report a heterostructure composed of Ni/Cu/TTLG/Cu/Ni where the TwR for parallel and anti-parallel configurations can reach up to 200% and 1600%, respectively. Those findings pave the way towards the integration of 2D materials in novel spinmechatronics based devices.

## ACKNOWLEDGMENTS

The authors would like to acknowledge Prof. Mairbek Chshiev and Dr. Fatima Ibrahim for the fruitful discussion and reviewing the manuscript. This project has received funding from the European Union Horizon 2020 research and innovation Programme under grant agreement No. 785219 (Graphene Flagship).

---

\* ali.hallal@hotmail.fr, ali.hallal@cea.fr

- [1] E. Cobas, A. L. Friedman, O. M. J. van't Erve, J. T. Robinson, and B. T. Jonker, *Nano Letters* **12**, 3000 (2012), pMID: 22577860.
- [2] A. K. Singh and J. Eom, *ACS Applied Materials & Interfaces* **6**, 2493 (2014), pMID: 24495123.
- [3] E. D. Cobas, O. M. J. van't Erve, S.-F. Cheng, J. C. Culbertson, G. G. Jernigan, K. Bussman, and B. T. Jonker, *ACS Nano* **10**, 10357 (2016), pMID: 27806204.
- [4] Y. Hu, M. Ji, J. Peng, W. Qiu, M. Pan, J. Zhao, Y. Yao, C. Han, J. Hu, L. Pan, W. Tian, D. Chen, Q. Zhang, and P. Li, *Journal of Magnetism and Magnetic Materials* **487**, 165317 (2019).
- [5] M. Piquemal-Banci, R. Galceran, F. Godel, S. Caneva, M.-B. Martin, R. S. Weatherup, P. R. Kidambi, K. Bouzehouane, S. Xavier, A. Anane, F. Petroff, A. Fert, S. M.-M. Dubois, J.-C. Charlier, J. Robertson, S. Hofmann, B. Dlubak, and P. Seneor, *ACS Nano* **12**, 4712 (2018), pMID: 29697954.
- [6] V. M. Karpan, G. Giovannetti, P. A. Khomyakov, M. Talanana, A. A. Starikov, M. Zwierzycki, J. van den Brink, G. Brocks, and P. J. Kelly, *Phys. Rev. Lett.* **99**, 176602 (2007).
- [7] K. K. Saha, A. Blom, K. S. Thygesen, and B. K. Nikolić, *Phys. Rev. B* **85**, 184426 (2012).
- [8] W. Qiu, J. Peng, M. Pan, Y. Hu, M. Ji, J. Hu, W. Tian, D. Chen, Q. Zhang, and P. Li, *Journal of Magnetism and Magnetic Materials* **476**, 622 (2019).
- [9] C. Vo-Van, Z. Kassir-Bodon, H. Yang, J. Coraux, J. Vogel, S. Pizzini, P. Bayle-Guillemaud, M. Chshiev, L. Ranno, V. Guisset, P. David, V. Salvador, and O. Fruchart, *New Journal of Physics* **12**, 103040 (2010).
- [10] N. Rougemaille, A. T. N'Diaye, J. Coraux, C. Vo-Van, O. Fruchart, and A. K. Schmid, *Applied Physics Letters* **101**, 142403 (2012), <https://doi.org/10.1063/1.4749818>.
- [11] J. Coraux, A. T. N'Diaye, N. Rougemaille, C. Vo-Van, A. Kimouche, H.-X. Yang, M. Chshiev, N. Bendiab, O. Fruchart, and A. K. Schmid, *The Journal of Physical Chemistry Letters* **3**, 2059 (2012).
- [12] H. Yang, A. D. Vu, A. Hallal, N. Rougemaille, J. Coraux, G. Chen, A. K. Schmid, and M. Chshiev, *Nano Letters* **16**, 145 (2016), pMID: 26641927.
- [13] H. Yang, G. Chen, A. A. C. Cotta, A. T. N'Diaye, S. A. Nikolaev, E. A. Soares, W. A. A. Macedo, K. Liu, A. K. Schmid, A. Fert, and M. Chshiev, *Nature materials* **17**, 605 (2018).
- [14] F. Ajejas, A. Gudín, R. Guerrero, A. Anadón Barcelona, J. M. Diez, L. de Melo Costa, P. Olleros, M. A. Niño, S. Pizzini, J. Vogel, M. Valvidares, P. Gargiani, M. Cabero, M. Varela, J. Camarero, R. Miranda, and P. Perna, *Nano Letters* **18**, 5364 (2018), pMID: 30052462.
- [15] A. K. Chaurasiya, A. Kumar, R. Gupta, S. Chaudhary, P. K. Muduli, and A. Barman, *Phys. Rev. B* **99**, 035402 (2019).
- [16] A. Barla, V. Bellini, S. Rusponi, P. Ferriani, M. Pivetta, F. Donati, F. Patthey, L. Persichetti, S. K. Mahatha, M. Papagno, C. Piamonteze, S. Fichtner, S. Heinze, P. Gambardella, H. Brune, and C. Carbone, *ACS Nano* **10**, 1101 (2016), pMID: 26588469.
- [17] P. Gargiani, R. Cuadrado, H. B. Vasili, M. Pruneda, and M. Valvidares, *Nature Communications* **8**, 699 (2017).
- [18] Y. Cao, V. Fatemi, S. Fang, K. Watanabe, T. Taniguchi, E. Kaxiras, and P. Jarillo-Herrero, *Nature* **556**, 43 (2018), 1803.02342 [cond-mat.mes-hall].

- [19] A. Kerelsky, L. J. McGilly, D. M. Kennes, L. Xian, M. Yankowitz, S. Chen, K. Watanabe, T. Taniguchi, J. Hone, C. Dean, A. Rubio, and A. N. Pasupathy, *Nature* **572**, 95 (2019).
- [20] G. Chen, A. L. Sharpe, P. Gallagher, I. T. Rosen, E. J. Fox, L. Jiang, B. Lyu, H. Li, T. Watanabe, K. and Taniguchi, J. Jung, Z. Shi, D. Goldhaber-Gordon, Y. Zhang, and F. Wang, *Nature* (2019).
- [21] H. Isobe, N. F. Q. Yuan, and L. Fu, *Phys. Rev. X* **8**, 041041 (2018).
- [22] Y. Cao, V. Fatemi, A. Demir, S. Fang, S. L. Tomarken, J. Y. Luo, J. D. Sanchez-Yamagishi, K. Watanabe, T. Taniguchi, E. Kaxiras, R. C. Ashoori, and P. Jarillo-Herrero, *Nature* **556**, 80 (2018), 1802.00553.
- [23] Y. Xie, B. Lian, B. Jack, X. Liu, C.-L. Chiu, K. Watanabe, T. Taniguchi, B. A. Bernevig, and A. Yazdani, *Nature* **572**, 101 (2019).
- [24] J. Kang and O. Vafek, *Phys. Rev. X* **8**, 031088 (2018).
- [25] M. Koshino, N. F. Q. Yuan, T. Koretsune, M. Ochi, K. Kuroki, and L. Fu, *Phys. Rev. X* **8**, 031087 (2018).
- [26] A. L. Sharpe, E. J. Fox, A. W. Barnard, J. Finney, K. Watanabe, T. Taniguchi, M. A. Kastner, and D. Goldhaber-Gordon, *Science* (2019), 10.1126/science.aaw3780.
- [27] J. Liu, Z. Ma, J. Gao, and X. Dai, *Phys. Rev. X* **9**, 031021 (2019).
- [28] R. Ribeiro-Palau, C. Zhang, K. Watanabe, T. Taniguchi, J. Hone, and C. R. Dean, *Science* **361**, 690 (2018).
- [29] M. Andelković, L. Covaci, and F. M. Peeters, *Phys. Rev. Materials* **2**, 034004 (2018).
- [30] T.-F. Chung, Y. Xu, and Y. P. Chen, *Phys. Rev. B* **98**, 035425 (2018).
- [31] E. H. Hwang and S. D. Sarma, *arxiv:1907.02856* (2019).
- [32] P. Brandimarte, M. Engelund, N. Papior, A. Garcia-Lekue, T. Frederiksen, and D. Sánchez-Portal, *The Journal of Chemical Physics* **146**, 092318 (2017).
- [33] W. Yao, E. Wang, C. Bao, Y. Zhang, K. Zhang, K. Bao, C. K. Chan, C. Chen, J. Avila, M. C. Asensio, J. Zhu, and S. Zhou, *Proceedings of the National Academy of Sciences* **115**, 6928 (2018).
- [34] E. Suárez Morell, M. Pacheco, L. Chico, and L. Brey, *Phys. Rev. B* **87**, 125414 (2013).
- [35] E. Artacho, D. Sánchez-Portal, P. Ordejón, A. García, and J. M. Soler, *physica status solidi (b)* **215**, 809 (1999).
- [36] J. M. Soler, E. Artacho, J. D. Gale, A. García, J. Junquera, P. Ordejón, and D. Sánchez-Portal, *Journal of Physics: Condensed Matter* **14**, 2745 (2002).
- [37] J. P. Perdew, K. Burke, and M. Ernzerhof, *Phys. Rev. Lett.* **77**, 3865 (1996).
- [38] M. Brandbyge, J.-L. Mozos, P. Ordejón, J. Taylor, and K. Stokbro, *Phys. Rev. B* **65**, 165401 (2002).
- [39] N. Papior, N. Lorente, T. Frederiksen, A. García, and M. Brandbyge, *Computer Physics Communications* **212**, 8 (2017).
- [40] M. B. Lim, R. G. Felsted, X. Zhou, B. E. Smith, and P. J. Pauzauskie, *Applied Physics Letters* **113**, 031106 (2018).
- [41] K. Wang, E. Schonbrun, P. Steinvurzel, and K. B. Crozier, *Nature Communications* **2**, 469 (2011).
- [42] O. M. Maragò, P. H. Jones, P. G. Gucciardi, G. Volpe, and A. C. Ferrari, *Nature Nanotechnology* **8**, 807 (2013).
- [43] M. F. Maghrebi, A. V. Gorshkov, and J. D. Sau, *Phys. Rev. Lett.* **123**, 055901 (2019).